

Comparison of adaptive uncertainty quantification approaches for shock wave-dominated flows

By D. Lucor^{†‡}, J. Witteveen, P. Constantine, D. Schiavazzi, AND G. Iaccarino

Shock wave-dominated systems are very sensitive to uncertainties in initial or boundary conditions as they often give rise to strong non-linear responses when subject to perturbations. As global numerical approximations are not well suited to capture local parametric front/shocks/gradients, several adaptive methods have been proposed in this stochastic context. In this paper, we review some of these non-intrusive methods by considering simple functional test cases and the more involved Woodward-Colella benchmark of a high-speed flow in a channel with a forward step that we expose to uncertainties in the upstream Mach number and the adiabatic coefficient of the fluid. This survey is not exhaustive but this preliminary work will help in understanding strengths and weaknesses of the different approaches in an effort to bridge the gap between them.

1. Introduction

While it is widely agreed that standard stochastic spectral methods, such as Polynomial Chaos (PC) and generalized Polynomial Chaos (gPC) approximations benefit from numerous advantages (Wiener 1938; Ghanem & Spanos 2003; Xiu & Karniadakis 2002), they also present some limitations for complex engineering applications with realistic uncertainty conditions. The main limitation is a high computational cost due to the “curse of dimensionality” (e.g. related to the correlation length of the process), which translates into the resolution of very large systems of equations or equivalently countless calls to the deterministic solver. The other limitation is the lack of robustness and accuracy for strongly non-linear systems for which stochastic global approximations are not well suited to capturing solution local parametric front/shocks/gradients. Obviously, these two points are often intricately connected, for most strongly non-linear engineering systems, such as non-linear fluid mechanics models that exhibit a steep or discontinuous response/transition to a smooth variation of the system inputs. In the study of compressible flows, uncertainty may creep from numerous sources: physical and computational domain and geometry (manufacturing process, roughness, domain size, boundary conditions, etc.), initial and operating conditions, physical and turbulence models, mathematical model assumptions/simplifications (e.g. linearization, adiabaticity, perfect gas, etc.), discretization and numerical algorithmic errors (round-off or truncation error, numerical dissipation/dispersion, aliasing, etc.). Despite real progress in the development of deterministic numerical schemes (Liska & Wendroff 2003), the presence of some latent uncertainty makes the characterization of the reliability of the output very difficult. The large variety of physical and stochastic flow scales in this case calls for *adaptive* numerical methods.

Different answers have been proposed to overcome these obstacles in the study of

[†] UPMC Univ Paris 06, Institut Jean Le Rond d’Alembert, F-75005 Paris, France

[‡] CNRS, UMR 7190, Institut Jean Le Rond d’Alembert, F-75005 Paris, France

compressible flows. Mathelin *et al.* (2005) have applied the Galerkin PC representation to quasi-one-dimensional supersonic nozzle flow with uncertainty in inlet conditions and geometry. Several works in the supersonic regime have been performed by Lin *et al.* (2006) dealing with 2D Euler equations for a stochastic wedge flow where they use a piecewise gPC approximations. Chantrasmi *et al.* (2009) introduce a non-intrusive global stochastic representation based on a Padé-Legendre formalism coupled to a filtering procedure to minimize the errors introduced in the approximation close to the discontinuities.

Abgrall (2008) and coworkers develop a non-intrusive numerical scheme based on ENO-like reconstructions in the stochastic space for the advection, Burgers, and Euler equations. It is based on a formulation reminiscent of what is done in finite volume schemes to compute a polynomial reconstruction in order to increase the computed flux accuracy via a MUSCL extrapolation. Later, they propose a semi-intrusive evolution that requires only a limited amount of modification in the deterministic flow (Abgrall *et al.* 2011). Poëtte *et al.* (2009, 2011) have proposed a stochastic intrusive approach to tackle shocks in compressible gas dynamics. Their gPC-based technique relies on the decomposition of the *entropic* variable of the flow and does not require a special discretization of the random space. More recently, Tryoen *et al.* (2010) also consider non-linear hyperbolic systems of conservation laws. Loeven *et al.* (2007) make use of a deterministic compressible Reynolds Averaged Navier Stokes (RANS) code, which is coupled to a probabilistic collocation solver to propagate free-stream aerodynamic uncertainty through a subsonic steady flow around an airfoil. Subsequently, Simon *et al.* (2010) conduct deeper investigations of stochastic transonic flows around an airfoil. They emphasize the stochastic interplay between the stochastic shock and separated shear-layers. Iaccarino *et al.* (2010) show that high-order expansions are required to capture the correct statistical moments of stochastic Riemann problem and Woodward-Colella forward step problem (Woodward & Colella 1984).

In this paper, we consider several non-intrusive stochastic spectral-based methods relying on black-box deterministic (CFD) solvers. The goal is to evaluate the efficiency of these discretizations in an effort to understand their connections to eventually improve and couple them in the future. Comparisons are carried out based on applications to mono- and multidimensional functional test cases. The methods that seem most promising are then employed for the uncertainty quantification of a more challenging sensitive CFD simulation involving stochastic compressible fluid dynamics.

2. Preliminary study

We investigate the relevance of a few adaptive non-intrusive stochastic representations on simple test cases. Straightforward comparisons in terms of accuracy versus computational cost are obviously difficult as the different methods are not always designed for the same purpose and do not bear the same type or level of adaptivity (e.g. sampling vs. approximation basis adaptivity).

In this study, we consider: (a) a Padé-Legendre approximation (PL) (Chantrasmi *et al.* 2009), which builds the unknown function as a rational function of Legendre polynomials, where the coefficients of the polynomial numerator and denominator are computed via Galerkin projection, (b) a Multi-Wavelets approach (MW) that adaptively seeks the sparser approximation according to a redundant Alpert multiwavelet dictionary, (c) a Simplex Stochastic Collocation (SSC) method (Witteveen & Iaccarino 2011) that discretizes the probability space using a simplex tessellation of sampling points and ap-

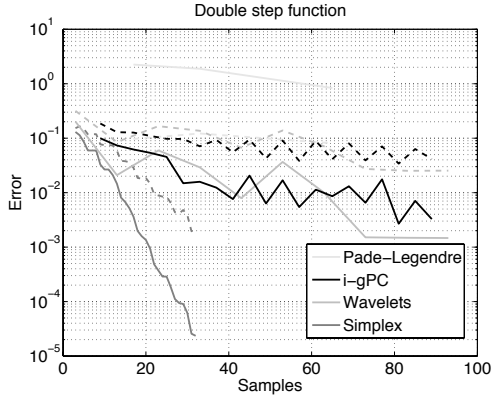


FIGURE 1. Convergence results for f_1 approximation. Solid lines: L^1 -norm; dashed lines: L^2 -norm.

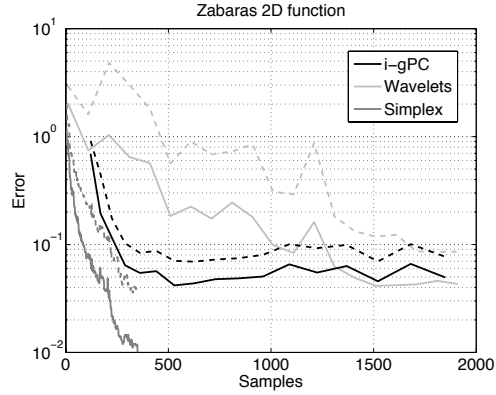


FIGURE 2. Convergence results for f_2 approximation. Solid lines: L^1 -norm; dashed lines: L^2 -norm.

proximates the response surface using higher-degree polynomial interpolation stencils of sampling points, (d) an iterative generalized Polynomial Chaos (i-gPC) (Poëtte & Lucor 2012) that automatically builds a recursive approximation based on an iterative adaptation of polynomial basis to the solution.

In the following, two types of test functions with discontinuities or discontinuous derivatives are investigated that require adaptive representations in order to avoid Gibbs-type oscillations. The first functional choice is $y = f_1(x)$, with x a *uniform* random variable $x \sim \mathcal{U}_{[-1,1]}$ and f_1 a double step function where the first discontinuity lies in $x = -0.4$ and the second one in $x = 0.6$ to make it non-symmetric. More specifically, we choose:

$$f_1(x) = \begin{cases} 1 & \text{for } -1 \leq x \leq -0.4, \\ 0.5, & \text{for } -0.4 \leq x < 0.6, \\ 0, & \text{otherwise.} \end{cases}$$

The second functional has two dimensions with a line singularity and takes the form (Ma & Zabaras 2009):

$$y = f_2(x_1, x_2) = \frac{1}{|0.3 - x_1^2 - x_2^2| + 0.1} \quad \text{with } (x_1, x_2) \sim \mathcal{U}_{[0,1] \times [0,1]}. \quad (2.1)$$

Convergence results in different error norms are presented in Figures 1 and 2 for the f_1 and f_2 functionals. The different approximation models are built from a “training” set made of a certain number of function samples (cf. horizontal axis), and are then tested and compared on an independent set of 10,000 Monte-Carlo points. The specific numerical setup for each method is not presented here. We notice that convergence is not always monotonic and sometimes stagnates for larger training data set. This is particularly true for methods relying on fixed structured sampling grids. The most efficient approach is the SSC method that iteratively and sequentially adapts the samples position based on Simplex refinements.

Our preliminary study suggests that SSC-SR & i-gPC are promising approaches despite being very different. In the following, we describe these two methods in more detail and apply them to a more challenging problem involving uncertain high speed compressible gas dynamics in a two-dimensional domain.

3. Retained adaptive numerical methods

In the following, we note $\boldsymbol{\xi}$ the *known* random vector of dimension n_ξ that belongs to a parametric space Ξ and the goal is to approximate a random variable $y = u(x, \boldsymbol{\xi})$, where u is a strongly non-linear transformation of $\boldsymbol{\xi}$ from a finite set of function evaluations $v_k(x) = u(x, \boldsymbol{\xi}_k)$ called samples. The spatial x coordinate will sometimes be dropped for simplicity.

3.1. Stochastic collocation with Simplex tessellation and subcell resolution

The Simplex Stochastic Collocation (SSC) method (Witteveen & Iaccarino 2012a,b) discretizes the parameter space using a tessellation of n_e non-overlapping simplexes Ξ_j , for which holds $\Xi = \bigcup_{j=1}^{n_e} \Xi_j$. The n_s sampling points $\boldsymbol{\xi}_k$ are located at the vertexes of the simplexes Ξ_j , for which the samples $v_k(x)$ are computed. The continuous response surface for $u(x, \boldsymbol{\xi})$ in the probability space is approximated by an interpolation $w(x, \boldsymbol{\xi})$ of the samples $\mathbf{v}(x) = \{v_1(x), \dots, v_{n_s}(x)\}$ using a PC expansion (Ghanem & Spanos 2003; Xiu & Karniadakis 2002) in each of the simplexes Ξ_j . A higher-degree approximation is obtained by interpolating the samples $v_k(x)$ of a stencil $S_j(x) = \{\boldsymbol{\xi}_{k_{j,0}}, \dots, \boldsymbol{\xi}_{k_{j,N_j(x)}}\}$ of $N_j(x) + 1$ unique sampling points $\boldsymbol{\xi}_k$, with $k_{j,l} \in \{1, \dots, n_s\}$ and $l = 0, \dots, N_j(x)$, that consist of the vertexes of the simplex Ξ_j and $N_j(x) - n_\xi$ vertexes of surrounding simplexes; See Figure 3 for an example in a two-dimensional probability space.

The subcell resolution variant of the SSC method (SSC-SR) (Witteveen & Iaccarino 2011) is applicable to problems with discontinuities in the physical space, of which the location $x_{\text{disc}}(\boldsymbol{\xi})$ is random. The first step of the algorithm extracts the n_s realizations $\mathbf{v}_{\text{disc}} = \{v_{\text{disc}_1}, \dots, v_{\text{disc}_{n_s}}\}$ for the physical discontinuity location $x_{\text{disc}}(\boldsymbol{\xi})$ from the samples $\mathbf{v}(x)$. These realizations at the sampling points $\boldsymbol{\xi}_k$ are interpolated over the probability space to the function $w_{\text{disc}}(\boldsymbol{\xi})$ using the SSC interpolation. This provides an approximation of the discontinuity location x_{disc} in the physical space as a function of the stochastic coordinates $\boldsymbol{\xi}$. The location of the discontinuity $\Xi_{\text{disc}}(x) \subset \Xi$ at a certain location x in the physical space is then given by the intersection of $w_{\text{disc}}(\boldsymbol{\xi})$ with the hyperplane $x_{\text{disc}}(\boldsymbol{\xi}) = x$, such that for all points $\boldsymbol{\xi}_{\text{disc}} \in \Xi_{\text{disc}}(x)$ holds $w_{\text{disc}}(\boldsymbol{\xi}_{\text{disc}}) = x$. The final step to reconstruct the truly discontinuous response surface is to extend the interpolations $w_i(\boldsymbol{\xi})$ in the neighboring simplexes Ξ_i from both sides into the discontinuous simplex Ξ_j up to the predicted discontinuity location $\Xi_{\text{disc}}(x)$ to replace $w_j(\boldsymbol{\xi})$; See Figure 4 for an example in a one-dimensional probability space. The method is directly applicable on a given arbitrary tessellation of the random space, or may be applied iteratively on successive tessellation levels based on some judicious refinement criteria. In this case, the scheme adapts both the samples set and the interpolation operator.

3.2. Iterative pseudospectral Polynomial Chaos approximation

Here, we briefly recall the main ingredients of the *iterative* approach for Galerkin-based spectral projection methods, named iterative-gPC (i-gPC) and that is well suited when non-linear transformations of random variables are in play, (Poëtte & Lucor 2012). A Lanczos approximation method is used to evaluate the adaptive polynomial basis instead of moments-based methods as proposed by the authors in their original formulation (Poëtte & Lucor 2012).

Suppose $\boldsymbol{\xi}$ denotes an input random vector, and one wants to approximate a random variable: $y = u(\boldsymbol{\xi})$ where u is a (possibly non-linear) transformation of $\boldsymbol{\xi}$.

The initial step of this non-linear approximation method is based on a standard pseu-

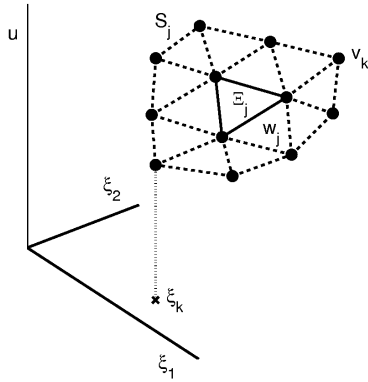


FIGURE 3. SSC response surface approximation.

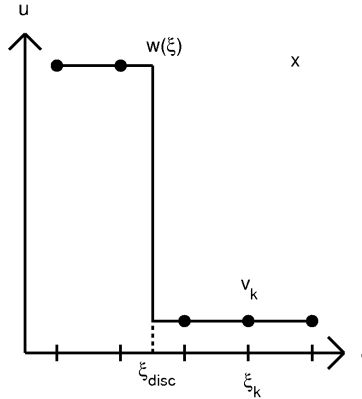


FIGURE 4. Subcell resolution.

dispectral gPC approximation of y :

$$y \approx y_{\xi}^P(\boldsymbol{\xi}) = \sum_{k=0}^P y_k^{\xi} \phi_k^{\xi}(\boldsymbol{\xi}) := z \tag{3.1}$$

with the moments of y in the P -truncated basis $(\phi_k^{\xi})_{k \in \{0, \dots, P\}}$ defined by

$$y_k^{\xi} = \mathbb{E}[u(\boldsymbol{\xi}) \phi_k^{\xi}(\boldsymbol{\xi})], \forall k \in \{0, \dots, P\}, \tag{3.2}$$

and evaluated thanks to numerical quadratures. We call z the P -terms gPC pseudospectral approximation of y .

Note that $P = P(Q, n_{\xi})$ depends on the dimension of $\boldsymbol{\xi}$ and the truncation order of the gPC representation in each dimensions Q . For example, for full tensorized product $P = Q^{n_{\xi}}$ or for triangular product $P = \frac{(Q+n_{\xi})!}{Q!n_{\xi}!}$, i.e. this dimensionality usually grows quickly.

Next, we look for a L^2 basis orthonormal $(\phi_k^z)_{k \in \mathbb{N}}$ with respect to the numerical approximation distribution of z . For a continuous measure, there exist several numerical algorithms for the construction of orthogonal polynomials, including the Stieltjes procedure and the (modified) Chebyshev algorithm (Gautschi 1996; Golub & Meurant 1994). The latter, used in (Poëtte & Lucor 2012), requires a high precision in the evaluation of the solution moments i.e. in the inner products of Eq. (3.2), which may not be reliable in the context of finite precision numerical integration. In fact, because we only rely on the discrete samplings of our unknown functional and wish to avoid a full evaluation of the associated distribution, it is more natural to consider the discrete measure counterpart of z and use a Lanczos' algorithm.

The Lanczos' algorithm may be slower than the Stieltjes procedure but bears good stability properties (Gautschi 1996; Golub & Meurant 1994). It iteratively generates a symmetric, tridiagonal matrix (the Jacobi matrix) and a sequence of mutually orthogonal vectors known as the Lanczos vectors. It was also shown to be related to approximate Stieltjes procedure with a discrete inner product (Golub & Meurant 1994; Constantine & Phipps 2012). In this work, we use such a numerical construction based on the original set of quadrature points and the algorithm directly provides the numerical values of the updated approximation basis at the quadrature points. Concerning the stopping

criteria, it is well known that due to finite precision the Lanczos vectors will eventually lose orthogonality after some number of iterations (Meurant & Strakos 2006). Here, we use the same technique as in (Constantine & Phipps 2012) following a measure of loss of orthogonality given a tolerance.

In a next step, we seek the gPC development of $y = u(\boldsymbol{\xi})$ in the new orthogonal basis ϕ_k^z , now optimal with respect to z . If we denote the transformation F that relates the RVs $\boldsymbol{\xi}$ and z , we have $\boldsymbol{\xi} = F(z) = F_{\boldsymbol{\xi}}^{-1}(F_z(z))$, where $F_{\boldsymbol{\xi}}$ and F_z are the cdf of $\boldsymbol{\xi}$ and z , respectively. Note that in practice, we never look for F . In the new basis, the new expansion coefficients are expressed as:

$$u_l^z = \mathbb{E}[u \Phi_l^z(z(\boldsymbol{\xi}))], \forall l \in \{0, \dots, R\}, \quad (3.3)$$

and may be evaluated with the same quadrature points as previously used. The number of terms R is much smaller for multi-dimensional problems, i.e., $R \ll P$. We may then write the approximation in the new basis as:

$$u \approx u_z^R = \sum_l u_l^z \Phi_l^z(z(\boldsymbol{\xi})). \quad (3.4)$$

This process may be arbitrarily reiterated m -times in a form of nested approximations:

$$u \approx u_{z^m}^{R^m} := z^m = \sum_l u_l^{z^m} \Phi_l^{z^m} \left(z^{m-1} \left(z^{m-2} (\dots (\boldsymbol{\xi})) \right) \right) \quad (3.5)$$

In (Poëtte & Lucor 2012), we prove the $L^2(\Omega)$ convergence and accuracy of the approximation with the new basis compared to the original basis.

We apply these methods to several test cases with different levels of regularity, dimensionality and complexity, and compare them in terms of computational cost with the classical approach.

4. Numerical results

In the following we consider the difficult case of a two-dimensional uncertain supersonic flow in a wind tunnel with a forward facing step. The computational domain is 1 length unit wide and 3 length units long. The step is 0.2 length units high and is located 0.6 length units from the left inlet boundary condition. The deterministic version of this benchmark was treated in the paper by (Woodward & Colella 1984) and the flow bears in this case strong reflecting shocks, see for instance the fluid density in Figure 5 for specific values of upstream Mach number M and γ -law gas value. The objective was then to characterize precisely the position of the shock waves at a particular instant of time after the impulsive start of the channel. The position of these shocks strongly depends on the correct characterization of the fluid as well as its upstream velocity as well.

4.1. Woodward-Colella test case

The unsteady high-speed compressible gas flow is governed by the Euler equations and the numerical solution is here obtained using a second-order finite volume spatial discretization (on a grid consisting of $\approx 16,000$ structured elements (Iaccarino *et al.* 2010)) and an explicit Runge-Kutta integration (Pecnik *et al.* 2012) combined with a non-intrusive automated scheduler on a parallel architecture. We assume now that both M and γ

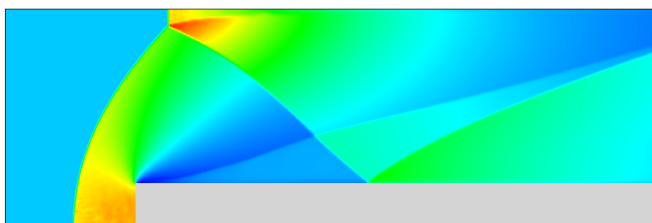


FIGURE 5. (Woodward & Colella 1984) forward facing step problem. Deterministic flow density field at $t = 2$ corresponding to Mach $M = 2.57$ and $\gamma = 1.4$.

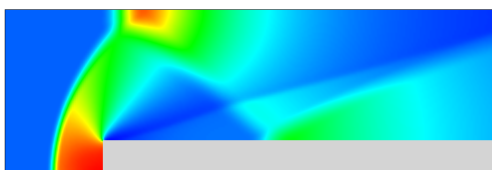


FIGURE 6. Mean pressure field for $M \sim \mathcal{U}_{[2.4565; 3.0551]}$ and $\gamma \sim \mathcal{U}_{[1.35; 1.45]}$.

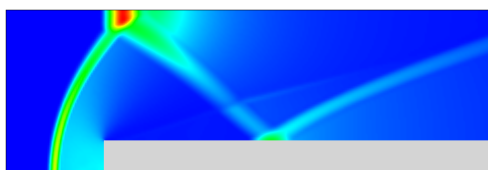


FIGURE 7. Std pressure field (same legend).

values are not well known in this experiment but are at least confined in finite ranges with *uniform* probability. The two parameters are specified as uniform random variables defined over the intervals $[2.4565; 3.0551]$ and $[1.35; 1.45]$ respectively.

A quick qualitative analysis of the solution moments – here from a stochastic collocation approximation on the most resolved grid CC_{332} – reveals the sensitive area of the flow. Figures 6 & 7 show mean and standard deviation (std) pressure fields respectively. As expected, the effect of the uncertainty is to smear the shock waves while strong std are present in sharp regions in the close vicinity of the shocks. Maximum std value is obtained at the upper wall slightly after the front of the step but a large value may be spotted as well along the step around $x \approx 1.7$.

In the following, we compare i-gPC and SSC-SR methods on the Woodward-Colella test case. In order to be fair, the computational grids used by both methods have the same number of points: 3^2 , 5^2 , 9^2 and 17^2 , and the flow fields are integrated up to the same final time $t = 2$. The i-gPC method relies on structured Clenshaw-Curtis (CC) grids while the SSC-SR method uses unstructured tessellation grids up to 17^2 vertices. The results are validated against data computed on a more refined CC_{332} grid. Ongoing work involving validation against Monte-Carlo simulations within the ranges of interest are currently underway. The quantities of interest are one-dimensional: the pressure and density along the upper part of the step, and two-dimensional: the pressure field in the entire domain.

Figures 8 and 9 compare the convergence rates of mean and std of the pressure field in L^1 - and L^2 -norm for SSC-SR & i-gPC (here the error norms are computed over the physical space, i.e. along the step). The horizontal axis represent the total number of samples (in both dimensions) required to construct the approximations. Both methods converge well and the results are similar for the SSC-SR and i-gPC. The same type of analysis was also performed for the density field. Nevertheless, the analysis is here slightly biased because the i-gPC method relies on CC grids that are subsets of the larger reference data set used to compute the error. The SSC-SR method, on the other hand, relies on an

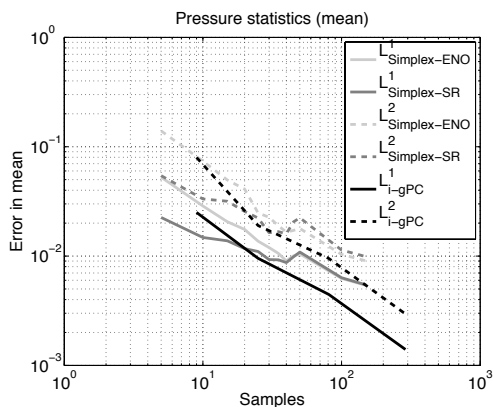


FIGURE 8. Convergence rates of pressure 1st moment measured along the step for SSC-SR & i-gPC.

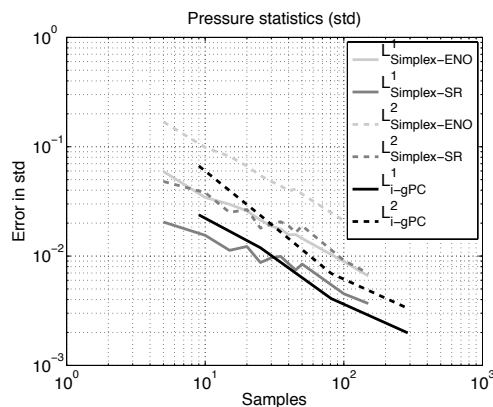


FIGURE 9. Convergence rates of pressure 2nd moment measured along the step for SSC-SR & i-gPC.

arbitrary tessellation of the random space. Convergence rates computed against Monte-Carlo simulations are the subject of current investigations and will be reported soon.

Figures 10-12 show attempts at computing the std of the pressure field in the domain – cf. reference results obtained from a Stochastic Collocation with 1,089 samples in Figure 10 – with very few samples and adaptive approaches. The SSC-SR method only uses 5 samples while i-gPC uses 4 additional samples (i.e. 3^2 CC grid points). The agreement is qualitatively acceptable. The former approach does very well where the shocks are weaker in the domain above the step. The latter does better in the front shock waves bow and with the shape of the large std spot at the top wall.

5. Summary

In this paper, we review and test some recent non-intrusive stochastic approximation methods. In particular we compare the Simplex Stochastic Collocation and the iterative generalized Polynomial Chaos methods on the Woodward-Colella benchmark of a high-speed flow over a forward step subject to uncertainties in the upstream Mach number and the adiabatic coefficient of the fluid. Both methods are robust and efficient enough to build an adaptive stochastic approximation at each point of the spatial domain. They do not degrade the accuracy of a standard generalized Polynomial Chaos approximation in regions of smooth response, and improve the results in regions dominated by shock waves. Good qualitative moments distributions are obtained with few samples compared to fully refined stochastic simulations.

Acknowledgments

The authors acknowledge CTR and HPCP at Stanford University for providing computing resources that have contributed to the research results reported within this report. The simulations have been performed on the computational cluster *Certainty*.

REFERENCES

ABGRALL, R. 2008 A simple, flexible and generic deterministic approach to uncertainty

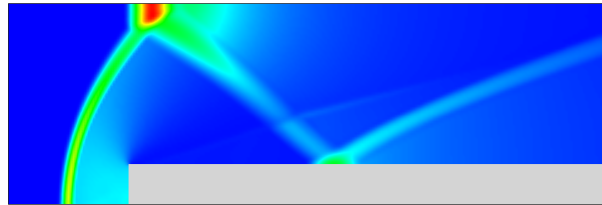


FIGURE 10. Std pressure field obtained from a stochastic collocation built on well-refined 33×33 Clenshaw-Curtis grid.

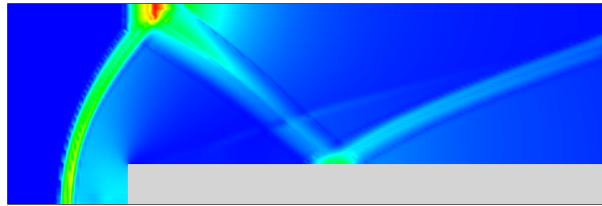


FIGURE 11. Std pressure field obtained from an adaptive SSC-SR approach built on coarse 5-point grid (corners + center points).



FIGURE 12. Std pressure field obtained from an adaptive i-gPC approach built on coarse 3×3 Clenshaw-Curtis grid (corners + center + mid-face points).

quantifications in non linear problems: application to fluid flow problems. *Rapport de Recherche INRIA* (00325315).

- ABGRALL, R., CONGEDO, P. M., GALERA, S. & GERACI, G. 2011 Semi-intrusive and non-intrusive stochastic methods for aerospace applications. In *4TH EUROPEAN CONFERENCE FOR AEROSPACE SCIENCES*. Saint Petersburg, Russia.
- CHANTRASMI, T., DOOSTAN, A. & IACCARINO, G. 2009 Padé-Legendre approximants for uncertainty analysis with discontinuous response surfaces. *J. of Computational Physics* **228** (19), 7159–7180.
- CONSTANTINE, P. G. & PHIPPS, E. T. 2012 A Lanczos method for approximating composite functions. *Applied Mathematics and Computation* **218** (24), 11751–11762.
- GAUTSCHI, W. 1996 Orthogonal polynomials: applications and computation. *Acta Numerica* **5**, 45–119.
- GHANEM, R. & SPANOS, P. 2003 *Stochastic Finite Elements: a Spectral Approach (revised edition)*. Springer-Verlag.
- GOLUB, G. H. & MEURANT, G. 1994 *Matrices, Moments and Quadrature with Applications*. Princeton University Press.
- IACCARINO, G., PETTERSSON, P., NORDSTROM, J. & WITTEVEEN, J. 2010 Numerical methods for uncertainty propagation in high speed flows. In *ECCOMAS CFD 2010*

- Proceedings of the V European Conference on Computational Fluid Dynamics* (ed. A. S. J. C. F. Pereira & J. M. C. Pereira). Lisbon, Portugal.
- LIN, G., SU, S.-H. & KARNIADAKIS, G. 2006 Predicting shock dynamics in the presence of uncertainties. *J. of Computational Physics* **217**, 260–276.
- LISKA, R. & WENDROFF, B. 2003 Comparison of Several Difference Schemes on 1D and 2D Test Problems for the Euler Equations. *SIAM J. on Scientific Computing* **25** (3), 995–1017.
- LOEVEN, G., WITTEVEEN, J. & BIJL, H. 2007 Probabilistic collocation: an efficient non-intrusive approach for arbitrarily distributed parametric uncertainties. AIAA Paper 2007–317.
- MA, X. & ZABARAS, N. 2009 An adaptive hierarchical sparse grid collocation algorithm for the solution of stochastic differential equations. *J. of Computational Physics* **228** (8), 3084–3113.
- MATHELIN, L., HUSSAINI, M. & ZANG, T. 2005 Stochastic approaches to uncertainty quantification in CFD simulations. *Numer. Algo.* **38**, 209–236.
- MEURANT, G. & STRAKOS, Z. 2006 The Lanczos and conjugate gradient algorithms in finite precision arithmetic. *Acta Numerica* **15**, 471–542.
- PECNIK, R., TERRAPON, V. E., HAM, F., IACCARINO, G. & PITSCH, H. 2012 Reynolds-Averaged Navier-Stokes Simulations of the HyShot II Scramjet. *AIAA Journal* **50** (8), 1717–1732.
- POËTTE, G., DESPRÉS, B. & LUCOR, D. 2009 Uncertainty quantification for systems of conservation laws. *J. of Computational Physics* **228** (7), 2443–2467.
- POËTTE, G., DESPRÉS, B. & LUCOR, D. 2011 Treatment of uncertain interfaces in compressible flows. *Comp. Meth. Appl. Math. Engrg.* **200** (1-4), 284–308.
- POËTTE, G. & LUCOR, D. 2012 Non intrusive iterative stochastic spectral representation with application to compressible gas dynamics. *J. of Computational Physics* **231** (9), 3587–3609.
- SIMON, F., GUILLEN, P., SAGAUT, P. & LUCOR, D. 2010 A gPC-based approach to uncertain transonic aerodynamics. *Comp. Meth. Appl. Math. Engrg.* **199** (17-20), 1091–1099.
- TRYOEN, J., LE MAÎTRE, O., NDJINGA, M. & ERN, A. 2010 Intrusive galerkin methods with upwinding for uncertain nonlinear hyperbolic systems. *J. of Computational Physics* **229**, 6485–6511.
- WIENER, N. 1938 The homogeneous chaos. *Amer. J. Math.* **60**, 897–936.
- WITTEVEEN, J. & IACCARINO, G. 2011 Introducing essentially non-oscillatory stencil selection with subcell resolution into uncertainty quantification. In *Annual Research Briefs, Center for Turbulence Research*, pp. 169–180. Stanford University.
- WITTEVEEN, J. & IACCARINO, G. 2012a Refinement criteria for simplex stochastic collocation with local extremum diminishing robustness. *SIAM J. on Scientific Computing* **34** (3), A1522–A1543.
- WITTEVEEN, J. & IACCARINO, G. 2012b Simplex stochastic collocation with random sampling and extrapolation for nonhypercube probability spaces. *SIAM J. on Scientific Computing* **34** (2), A814–A838.
- WOODWARD, P. & COLELLA, P. 1984 The numerical simulation of two-dimensional fluid flow with strong shocks. *J. of Computational Physics* **54** (1), 115–173.
- XIU, D. & KARNIADAKIS, G. 2002 The Wiener-Askey polynomial chaos for stochastic differential equations. *SIAM J. on Scientific Computing* **24** (2), 619–644.